Current Journal of Engineering and Science Research
Volume 3, Issue 11, pp 16-25, November 2026
ISSN (online): 3049-1738
DOI: https://doi.org/10.47001/CJESR/2026.311003
Available Online at https://www.cjesr.com

CFD Investigation of the Effects of Wind Speed and Duct Geometry on the Performance of a Ducted Wind Turbine for Energy Efficiency

[1]*Nazaruddin Sinaga, [2]Dwi Basuki Wibowo, [3]Rendy Augustino Sam

[1,2,3]Department of Mechanical Engineering, Faculty of Engineering, Diponegoro University, Semarang, Indonesia
Corresponding Author's E-mail: nsinaga19.undip@gmail.com

Abstract: Indonesia holds considerable wind energy potential, yet its prevailing wind speeds of roughly 2–6 m/s make it difficult for conventional turbines to operate near their optimum. Diffuser-augmented (ducted) wind turbines offer a promising remedy by accelerating the flow through the rotor plane. This study uses computational fluid dynamics (CFD) to examine how inlet wind speed, diffuser expansion ratio (ER), and relative flow rate affect the torque, power, and power coefficient of a ducted horizontal-axis wind turbine. Steady-state simulations were performed in ANSYS Fluent with a pressure-based solver, the k–ω SST turbulence model, and the Multiple Reference Frame (MRF) approach. The model was validated against published data at 4.5 m/s, with deviations of about 9.4% in torque and power. Raising the wind speed from 3 to 20 m/s increased the power output from 30.23 W to 139.87 W, while increasing ER from 1.0 to 2.5 raised it from 28.99 W to 35.79 W, with the gains flattening beyond ER = 2.0. Scaling the flow rate from 0.4Q to 1.6Q increased power from 28.06 W to 39.43 W but sharply reduced the power coefficient, revealing a trade-off between power output and conversion efficiency. Because the rotor speed was held constant, the effective tip speed ratio changed across the cases, which largely explains these trends. Within the ranges studied, wind speed was the dominant influence on power output, and a larger expansion ratio further improved energy extraction, supporting the use of diffusers in low-to-moderate wind regimes.

Keywords: Ducted wind turbine; diffuser-augmented wind turbine; expansion ratio; computational fluid dynamics; power coefficient; wind energy; low wind speed.

I. INTRODUCTION

The global transition toward renewable energy is a central strategy for reducing dependence on fossil fuels and curbing greenhouse gas emissions. Among the available options, wind power has grown especially quickly: cumulative installed capacity reached approximately 1,136 GW worldwide by the end of 2024 [1], and wind continues to be regarded as a key contributor to sustainable development [2], [3]. Indonesia has likewise set out to expand its renewable energy share, including a target of 7.2 GW of new wind capacity over 2025–2034 under its electricity supply plan [4].

Despite this ambition, wind remains under-used in Indonesia. The national wind potential is estimated at 154.9 GW, whereas the installed capacity stands at only about 157 MW [5]. A major reason is that wind speeds across much of the archipelago are low, typically 2–6 m/s [5]. Under such conditions, conventional turbines rarely reach their rated operating point, and the power they deliver is correspondingly modest.

The underlying physics explains why. The power that a conventional rotor can extract is bounded by the Betz limit, 59.3% of the kinetic power carried by the incoming wind [6], and that available power scales with the cube of the wind speed [6]. Even a small increase in the velocity at the rotor plane therefore yields a disproportionately large gain in power. This has motivated flow-augmentation devices that raise the rotor-plane velocity without requiring a stronger ambient wind.

One of the most widely studied devices is the ducted wind turbine, also known as the diffuser-augmented wind turbine (DAWT). A diffuser placed around the rotor creates a low-pressure region at its outlet; the resulting pressure difference draws more air through the rotor, so the flow at the rotor plane is

Copyright © 2026 CJESR All Rights Reserved

Current Journal of Engineering and Science Research
Volume 3, Issue 11, pp 16-25, November 2026
ISSN (online): 3049-1738
DOI: https://doi.org/10.47001/CJESR/2026.311003
Available Online at https://www.cjesr.com

faster than the free stream [7], [8]. A key geometric parameter is the expansion ratio (ER), defined as the ratio of the diffuser outlet area to its inlet area. A larger ER can accelerate the flow further, but beyond a certain point it promotes flow separation, which erodes performance [7], [8].

Computational fluid dynamics (CFD) is well suited to this problem because it reveals the flow field in fine detail at a lower cost than experiments [7]. In this paper, we use CFD to study how wind speed, diffuser expansion ratio, and flow rate jointly shape the performance of a ducted wind turbine. Section II reviews related work, Section III states the problem, Section IV describes the methodology, Section V presents and discusses the results, and Sections VI and VII provide conclusions and directions for future work.

II. LITERATURE SURVEY

A substantial body of research has shown that diffusers can improve turbine performance. Bekele and Bogale [9] carried out a parametric study of a diffuser for horizontal-axis wind turbine power augmentation, including the role of the flange. Sridhar *et al.* [10] compared slotted and non-slotted diffuser casings using three-dimensional CFD validated experimentally and reported that the slotted configuration improved the performance parameters by 27.4% over the non-slotted diffuser and by 46.8% over an open (bare) turbine at the tip speed examined. Numerical and experimental work on a ducted micro-scale turbine by Rahmatian *et al.* [11], together with the parametric study of a ducted micro wind energy harvester by Kim *et al.* [12], points in the same direction: a well-designed duct improves the aerodynamic performance of small turbines.

The most recent benchmark for the present work is the study by Teklemariyem *et al.* [7], who optimized a corrugated-flange diffuser integrated with a horizontal-axis turbine for low-wind conditions using ANSYS Fluent and the k–ω SST model. They reported a flow-velocity increase of 67.85% and a power coefficient of 0.524 for the integrated configuration. Their rotor (NACA 0012 profile, 0.7 m diameter) and operating point (4.5 m/s, tip speed ratio of 3) provide the geometry and reference data adopted in our model validation.

Other investigations have examined how duct design choices affect performance. Nile *et al.* [13] analyzed a small-scale diffuser-augmented turbine with and without an inlet nozzle in two and three dimensions, and Firoozi *et al.* [14] reviewed aerodynamic optimization in wind turbine blade design. Further numerical studies have considered shroud profiles [15], the divergence angle of flanged diffusers [16], the optimization of flanged diffusers for small-scale applications [17], and the effect of duct shape and size [18]. Taken together, these studies establish that diffuser geometry strongly governs flow augmentation, and that steady-state CFD with k–ω SST turbulence modeling is a standard, practical tool for exploring it.

III. PROBLEM DEFINITION

Most earlier CFD studies of ducted turbines concentrate on diffuser geometry at a single wind speed, and, to the best of our knowledge, comparatively few have examined the combined influence of wind speed, expansion ratio, and flow rate on torque, power, and power coefficient within one consistent numerical framework. Designers who want to deploy ducted turbines in low-to-moderate wind regions need this information to judge how much is gained from a larger diffuser and how the turbine behaves away from its design point.

The objective of this work is therefore to quantify, by CFD, the effects of (i) inlet wind speed from 3 to 20 m/s, (ii) diffuser expansion ratio from 1.0 to 2.5, and (iii) relative flow rate from 0.4Q to 1.6Q on the torque, power, and power coefficient (C_P) of a ducted horizontal-axis wind turbine, and to interpret the associated velocity fields. The study is limited to steady-state, incompressible, isothermal flow for a single benchmark rotor and diffuser geometry taken from [7].

IV. METHODOLOGY

A. Theoretical Background

The kinetic power available in a wind stream passing through a rotor swept area A is

$$P_{wind} = \tfrac{1}{2}\rho A V^3 \qquad (1)$$

where ρ is the air density (kg/m^3), A is the swept area (m^2), and V is the free-stream wind speed (m/s). Equation (1) shows that available power grows with V^3, so even modest changes in velocity have a large effect. The turbine performance is expressed by the power coefficient,

$$C_P = \frac{P_{turbine}}{\tfrac{1}{2}\rho A V^3} \qquad (2)$$

and the tip speed ratio (TSR) relates the blade tip speed to the wind speed,

Copyright © 2026 CJESR All Rights Reserved

Current Journal of Engineering and Science Research
Volume 3, Issue 11, pp 16-25, November 2026
ISSN (online): 3049-1738
DOI: https://doi.org/10.47001/CJESR/2026.311003
Available Online at https://www.cjesr.com

$$\lambda = \frac{\omega R}{V} \quad (3)$$

where ω is the rotor angular speed (rad/s) and R is the rotor radius (m). The turbine power is obtained from the computed torque T as

$$P_{turbine} = T\,\omega \quad (4)$$

Because the Betz limit applies to a free rotor in an unconfined stream tube, a ducted turbine whose C_P is referenced to the rotor swept area and the free-stream velocity can exceed 0.593 without violating any physical law; the diffuser increases the mass flow through the rotor. To allow comparison with the benchmark, we also report a second coefficient based on a diffuser reference area A_d,

$$C_{P,d} = \frac{P_{turbine}}{\frac{1}{2}\rho A_d V^3} \quad (5)$$

where A_d is the reference area based on the outer diameter of the diffuser (the tabulated coefficients imply $A_d \approx 1.57$ m², about 4.08 times the rotor area).

Steady, incompressible, isothermal flow is governed by the continuity and momentum equations [19],

$$\nabla \cdot (\rho \vec{V}) = 0 \quad (6)$$

$$\rho(\vec{V} \cdot \nabla)\vec{V} = -\nabla P + \mu \nabla^2 \vec{V} \quad (7)$$

where V is the velocity vector, P is the pressure, and μ is the dynamic viscosity. Turbulence was modeled with the k–ω SST (Shear Stress Transport) model [20], which blends the near-wall strength of the k–ω formulation with the free-stream behavior of the k–ε formulation and predicts adverse-pressure-gradient separation, such as that inside a diffuser, reliably. Rotor rotation was represented with the Multiple Reference Frame (MRF) method.

B. Research Workflow

The workflow is summarized in Fig. 1. The study began with a literature review and the collection of geometric and operating data for the reference turbine and diffuser [7]. A three-dimensional model was built in SolidWorks, meshed, and set up in ANSYS Fluent with boundary conditions and solver parameters. After the model was validated against the reference data at 4.5 m/s, parametric simulations were carried out for wind speed, expansion ratio, and flow rate, and the results were analyzed to identify how each parameter influences turbine performance.

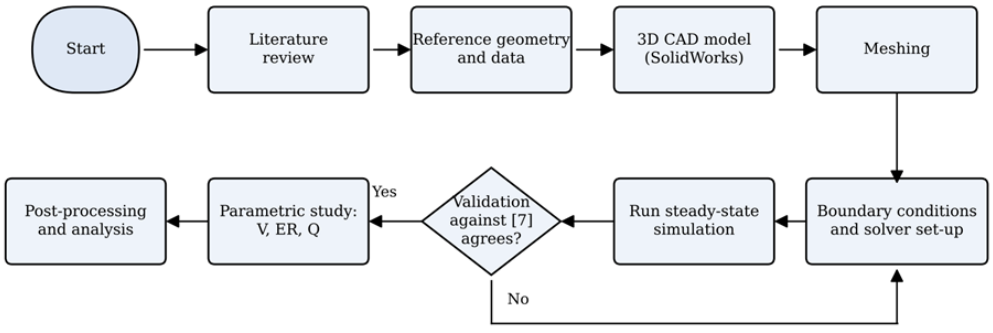


Figure 1: Research workflow

C. Geometry and Computational Domain

The turbine and diffuser follow the model of Teklemariyem *et al.* [7]: a horizontal-axis rotor with NACA 0012 blades (Table I) surrounded by a flanged diffuser. The rotor diameter is 0.70 m (R = 0.35 m) and the diffuser inlet diameter is D = 0.72 m. The expansion ratio was varied by changing the outlet diameter D_o = $D\sqrt{ER}$ while keeping the diffuser length fixed at 0.90 m, so the opening angle β increases with ER, from 0° at ER = 1.0 to 2.2°, 4.2°, 6.1°, 7.8°, 9.4°, and 13.1° at ER = 1.2, 1.4, 1.6, 1.8, 2.0, and 2.5, respectively. The three-dimensional model was built in SolidWorks and imported into ANSYS Fluent; a full 3D model was chosen so that the asymmetric flow around the rotating

Copyright © 2026 CJESR All Rights Reserved

Current Journal of Engineering and Science Research
Volume 3, Issue 11, pp 16-25, November 2026
ISSN (online): 3049-1738
DOI: https://doi.org/10.47001/CJESR/2026.311003
Available Online at https://www.cjesr.com

blades is captured.

Table I: Geometry of the rotor and diffuser

Parameter	Symbol	Value
Rotor diameter	D_r	0.70 m
Blade profile	–	NACA 0012
Average chord length	C_{avg}	0.108 m
Diffuser inlet diameter	D	0.72 m
Diffuser length	L	0.90 m (1.25 D)
Diffuser wall thickness	t	5 mm
Flange length	L_f	0.216 m (0.3 D)
Flange angle	φ	15°
Flange height	H	0.209 m
Blade-tip gap	–	0.01 m

The computational domain is a cylindrical enclosure 15.27D long and 11.89D in diameter, following the approach of [7], with the rotor–diffuser assembly placed 4.167D from the inlet. It is divided into a cylindrical rotating zone around the rotor and a stationary zone containing the rest of the domain (Fig. 2).

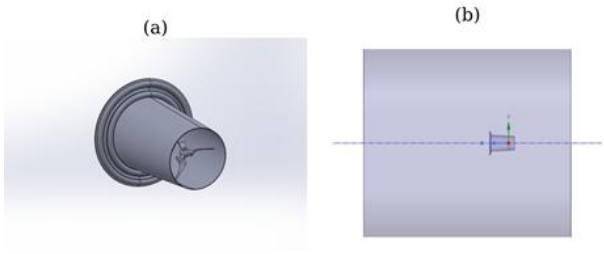


Figure 2: Model geometry: (a) three-dimensional geometry; (b) computational domain

D. Meshing, Boundary Conditions, and Solver Settings

A hybrid mesh was used: structured away from the turbine–diffuser assembly and unstructured around it, with face sizing and inflation layers along the blade and diffuser walls to resolve the near-wall flow. The mesh contains 2,234,521 elements, with a maximum skewness of 0.335, an average skewness of 0.0103, a minimum orthogonal quality of 0.20, and a maximum aspect ratio of 73.6.

Simulations were run in ANSYS Fluent with a steady-state, pressure-based solver for incompressible, isothermal flow, the k–ω SST model, and MRF. Pressure–velocity coupling used the SIMPLE scheme; gradients were evaluated by the least-squares cell-based method, pressure was discretized with a second-order scheme, and momentum, turbulent kinetic energy, and specific dissipation rate with second-order upwind schemes. The solution was initialized with hybrid initialization and run for 500–1000 iterations. A velocity inlet was imposed at the domain inlet and a pressure outlet at its exit; the blades and hub were set as moving walls rotating with the rotating zone, and all other walls were stationary no-slip walls. The inlet turbulence intensity was 5% with a turbulent viscosity ratio of 10 (Table II).

The following parameters were varied: wind speed (3, 5, 7, 10, 12, 15, and 20 m/s), diffuser expansion ratio (1.0, 1.2, 1.4, 1.6, 1.8, 2.0, and 2.5), and relative flow rate Q/Q_{design} (0.4, 0.6, 0.8, 1.0, 1.2, 1.4, and 1.6). The expansion-ratio series was simulated at the baseline velocity of 4.5 m/s. The flow rate was varied by scaling the inlet velocity relative to the baseline, with Q_{design} = 4.5 m/s × 0.385 m^2 = 1.732 m^3/s, so that 0.4–1.6Q_{design} corresponds to equivalent velocities of 1.8–7.2 m/s.

The rotor speed was kept at ω = 38.57 rad/s in all simulations, the value giving the design TSR of 3 at 4.5 m/s. Consequently, the effective TSR equals the design value only near the baseline velocity: it varies from 4.5 at 3 m/s to 0.67 at 20 m/s in the wind-speed series, and from 7.5 to 1.9 over the flow-rate series.

Table II: Operating parameters and boundary conditions

Parameter	Symbol	Value	Unit
Air density	ρ	1.225	kg/m^3
Dynamic viscosity	μ	1.825×10^{-5}	kg/(m·s)
Baseline wind speed	V	4.5	m/s
Design tip speed ratio	λ	3	–
Rotor angular speed	ω	38.57	rad/s
Turbulence intensity	I	5	%
Turbulent viscosity ratio	–	10	–
Turbulence model	–	k–ω SST	–
Solver type	–	Pressure-based	–

E. Model Validation Approach

The model was validated by comparing the simulated torque, power, and power coefficient with the reference data of Teklemariyem *et al.* [7] at 4.5 m/s and λ = 3. The model was considered adequate for parametric analysis if the deviation from the reference was below 10%.

Copyright © 2026 CJESR All Rights Reserved

Current Journal of Engineering and Science Research
Volume 3, Issue 11, pp 16-25, November 2026
ISSN (online): 3049-1738
DOI: https://doi.org/10.47001/CJESR/2026.311003
Available Online at https://www.cjesr.com

V. RESULTS AND DISCUSSION

A. Model Validation

Table III compares the simulation with the reference data. The torque deviates by 9.42%, the power by 9.38%, and the rotor-based power coefficient by 9.50%, all below 10%, a level commonly accepted for CFD validation. The remaining difference is plausibly due to mesh density, boundary-layer resolution, and the steady-state assumption, which the reference study also identifies as a limitation. The coefficient values exceed unity because C_P is referenced to the rotor swept area and the free-stream velocity (Section IV-A).

The diffuser-based coefficient differs more (28.25%): 0.376 here versus 0.524 in [7]. This gap largely reflects the air density: the present study uses $\rho = 1.225$ kg/m^3 (sea level), whereas [7] used $\rho = 0.97$ kg/m^3. Because the available power is proportional to density, rescaling the reference value to $\rho = 1.225$ kg/m^3 gives about 0.415, which reduces the deviation to about 9.4%, consistent with the other quantities. Validation nevertheless covers a single operating point.

Table III: Validation results at 4.5 m/s

Quantity	Simulation	Reference [7]	Deviation
Torque (N·m)	0.8536	0.9424	9.42%
Power (W)	32.93	36.34	9.38%
C_P (rotor)	1.533	1.694	9.50%
$C_{P,d}$ (diffuser)	0.376	0.524	28.25%

B. Effect of Wind Speed

Table IV and Fig. 3 give the results for wind speeds of 3–20 m/s. The torque increased from 0.7838 to 3.6264 N·m and the power from 30.23 to 139.87 W. Although the available wind power rises by a factor of about 296 over this range, the extracted power increases only about 4.6 times, because the rotor speed was held constant: the effective TSR falls from 4.5 to 0.67, so the rotor moves progressively away from its design point. As a result, the rotor-based power coefficient declines from 4.75 at 3 m/s to 0.074 at 20 m/s, and the diffuser-based coefficient from 1.165 to 0.018.

Table IV: Results for varying wind speed (ω = 38.57 rad/s)

V (m/s)	Torque (N·m)	Power (W)	TSR	C_P (rotor)	$C_{P,d}$ (diffuser)
3	0.7838	30.23	4.50	4.750	1.165
5	0.8784	33.88	2.70	1.150	0.282
7	1.0008	38.60	1.93	0.477	0.117
10	1.3773	53.12	1.35	0.225	0.055
12	1.7062	65.81	1.12	0.162	0.040
15	2.3180	89.41	0.90	0.112	0.028
20	3.6264	139.87	0.67	0.074	0.018

The very high coefficients at low speed arise because the rotor turns at a TSR far above its design value while the available power in the denominator is small; they should be read as indicators of extreme off-design operation rather than as actual conversion efficiencies. The operating condition closest to the design point lies at roughly 4.5–7 m/s, where the TSR is about 1.9–3 and the rotor-based C_P ranges from 1.53 to 0.48. In this window the rotor rotates at a speed appropriate to the flow, whereas at high wind speed (TSR < 1) the rotor turns too slowly relative to the flow and much of the kinetic energy passes through without being extracted.

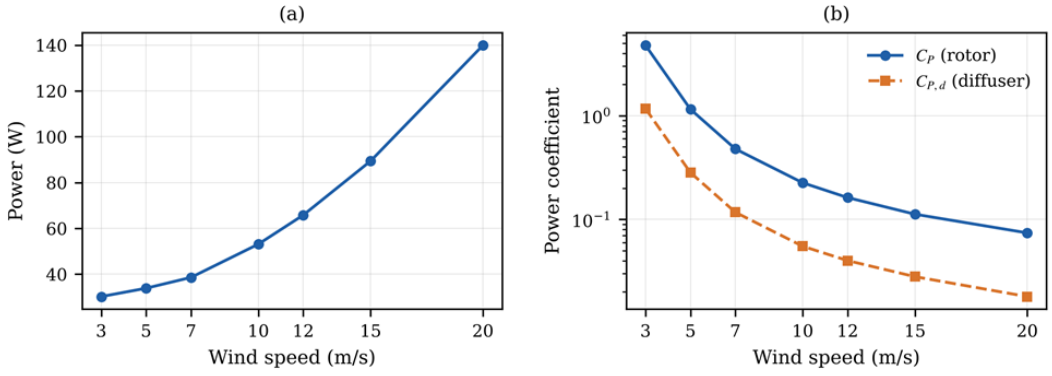


Figure 3: Effect of wind speed on (a) power and (b) power coefficient (logarithmic scale)

Copyright © 2026 CJESR All Rights Reserved

Current Journal of Engineering and Science Research
Volume 3, Issue 11, pp 16-25, November 2026
ISSN (online): 3049-1738
DOI: https://doi.org/10.47001/CJESR/2026.311003
Available Online at https://www.cjesr.com

The velocity contours in Fig. 4 show that the flow accelerates as it passes through the diffuser, with the highest velocity concentrated around the rotor plane inside the diffuser. This pattern is consistent across all wind speeds, which confirms that the flow-augmentation mechanism remains active over the whole range. A low-velocity wake and recirculation region forms behind the flange; the resulting low pressure at the diffuser exit strengthens the acceleration at the rotor plane.

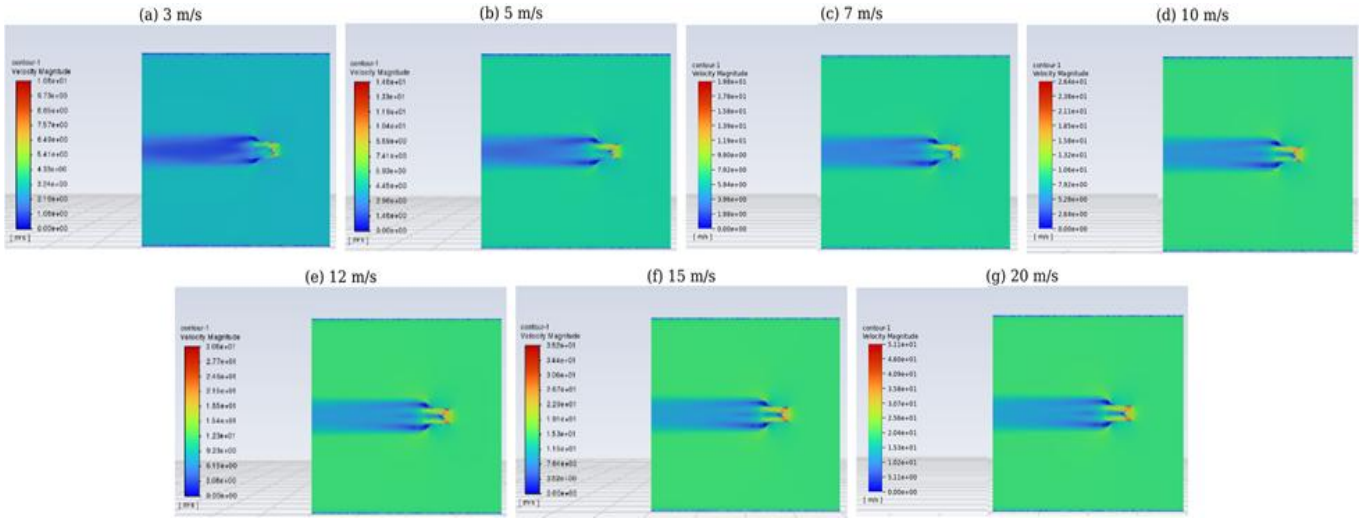


Figure 4: Velocity contours at different wind speeds: (a) 3, (b) 5, (c) 7, (d) 10, (e) 12, (f) 15, and (g) 20 m/s

C. Effect of Expansion Ratio

Table V and Fig. 5 show the effect of ER at 4.5 m/s. Increasing ER from 1.0 to 2.5 raised the torque from 0.7516 to 0.9278 N·m, the power from 28.99 to 35.79 W (+23.5%), the rotor-based C_P from 1.350 to 1.666, and the diffuser-based $C_{P,d}$ from 0.331 to 0.409. A larger outlet area strengthens the pressure drop on the downstream side, which draws more mass flow through the rotor and raises the local velocity at the rotor plane; the rotor can then extract more kinetic energy.

Table V: Simulation results for varying ER at 4.5 m/s

ER	Torque (N·m)	D_o (m)	Power (W)	C_P (rotor)	$C_{P,d}$
1.0	0.7516	0.720	28.99	1.350	0.331
1.2	0.7995	0.789	30.84	1.436	0.352
1.4	0.8308	0.852	32.04	1.492	0.366
1.6	0.8953	0.911	34.53	1.608	0.394
1.8	0.9143	0.966	35.26	1.642	0.403
2.0	0.9268	1.018	35.74	1.664	0.408
2.5	0.9278	1.138	35.79	1.666	0.409

The improvement, however, levels off. Between ER = 1.0 and 2.0 the power increases by 23.3%, whereas from ER = 2.0 to 2.5 it increases by only 0.14% (the torque differs by merely 0.001 N·m). The performance therefore saturates at about ER = 2.0. The contours in Fig. 6 support this reading: at ER = 2.0 and 2.5 (opening angles of 9.4° and 13.1°) a low-velocity region appears near the outlet wall of the diffuser, which suggests the onset of flow separation under a strong adverse pressure gradient. This agrees with the existence of an optimum opening angle reported in [7], [8]. Note that ER = 1.0 is a straight duct rather than a bare turbine, so the gains quoted here are relative to the straight duct.

Copyright © 2026 CJESR All Rights Reserved

Current Journal of Engineering and Science Research
Volume 3, Issue 11, pp 16-25, November 2026
ISSN (online): 3049-1738
DOI: https://doi.org/10.47001/CJESR/2026.311003
Available Online at https://www.cjesr.com

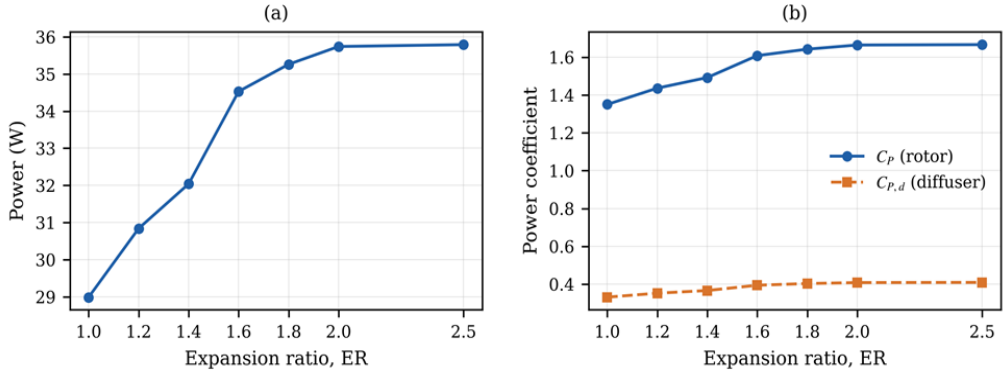


Figure 5: Effect of expansion ratio on (a) power and (b) power coefficient

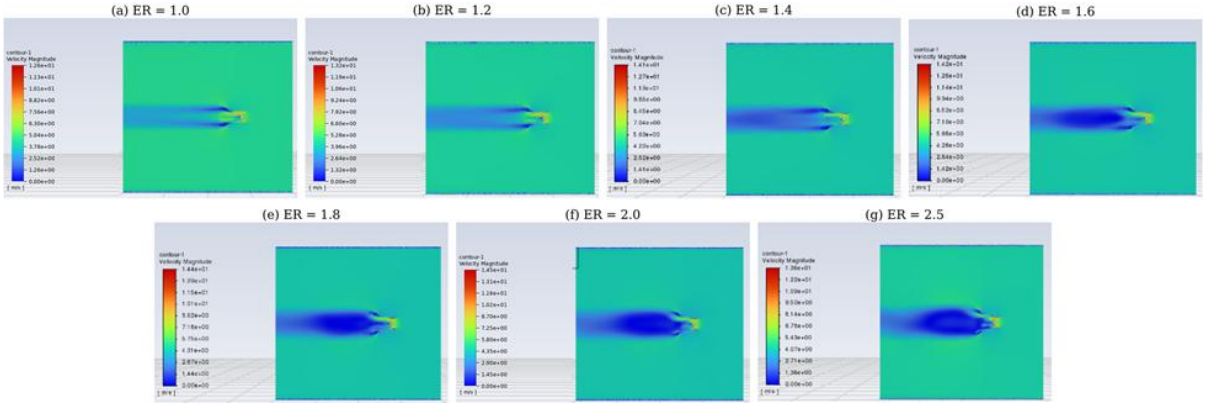


Figure 6: Velocity contours for different expansion ratios: (a) 1.0, (b) 1.2, (c) 1.4, (d) 1.6, (e) 1.8, (f) 2.0, and (g) 2.5

D. Effect of Flow Rate

The flow-rate series represents the low-wind regime that is most relevant to Indonesia, with equivalent velocities of 1.8–7.2 m/s (Table VI). Increasing Q/Q_{design} from 0.4 to 1.6 raised the torque from 0.7275 to 1.0223 N·m and the power from 28.06 to 39.43 W (+40.5%) (Fig. 7a). More flow through the rotor increases the available kinetic energy and the aerodynamic force on the blades, and therefore the torque and power. The values are close to those of the wind-speed series at comparable velocities, as expected because both series use the same rotor speed; this series simply refines the resolution at low velocity.

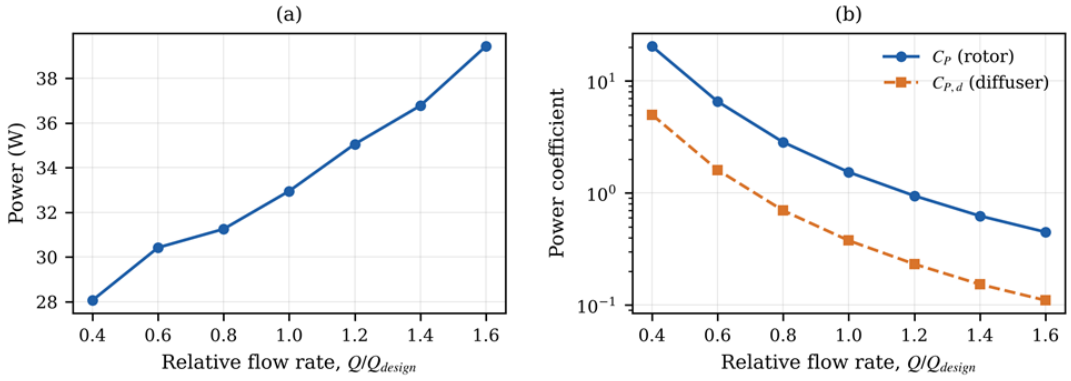


Figure 7: Effect of relative flow rate on (a) power and (b) power coefficient (logarithmic scale)

Copyright © 2026 CJESR All Rights Reserved

Current Journal of Engineering and Science Research
Volume 3, Issue 11, pp 16-25, November 2026
ISSN (online): 3049-1738
DOI: https://doi.org/10.47001/CJESR/2026.311003
Available Online at https://www.cjesr.com

In contrast, the power coefficient decreases sharply (Fig. 7b): the diffuser-based $C_{P,d}$ falls from 5.006 at 0.4Q to 0.110 at 1.6Q, and the rotor-based C_P from 20.4 to 0.448. Quadrupling the velocity raises the available power 64-fold but the extracted power by only 1.4 times, so relative conversion effectiveness drops even as absolute power rises. Two factors act together. At very low velocity the available power is tiny, which inflates the ratio, and the TSR is far above the design value (7.5 at 0.4Q), so the rotor operates in an extreme off-design condition. The more meaningful coefficients are found at 1.0–1.6Q (4.5–7.2 m/s), where the TSR is between 3 and 1.9 and the rotor-based C_P lies between 1.53 and 0.45. A higher flow rate therefore does not necessarily mean higher efficiency, and the operating point must balance power output against conversion efficiency. A more accurate coefficient would require the local velocity at the rotor plane rather than the free-stream velocity. The velocity fields appear in Fig. 8.

Table VI: Results for varying relative flow rate

Q/Q_{design}	Torque (N·m)	V (m/s)	Power (W)	C_P (rotor)	$C_{P,d}$
0.4	0.7275	1.80	28.06	20.411	5.006
0.6	0.7888	2.70	30.42	6.557	1.608
0.8	0.8103	3.60	31.25	2.842	0.697
1.0	0.8543	4.50	32.95	1.534	0.376
1.2	0.9087	5.40	35.05	0.944	0.232
1.4	0.9532	6.30	36.77	0.624	0.153
1.6	1.0223	7.20	39.43	0.448	0.110

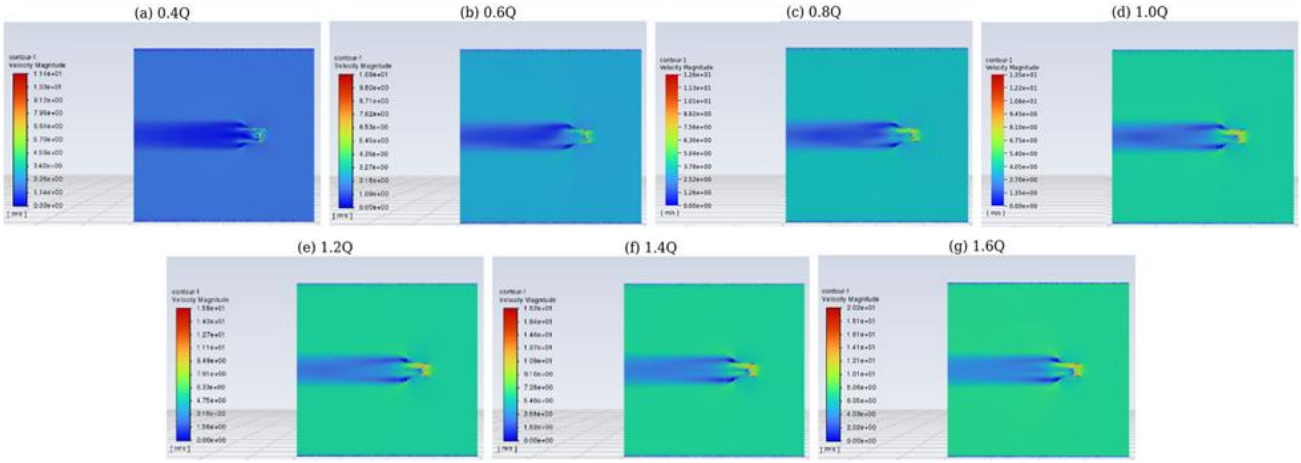


Figure 8: Velocity contours for different relative flow rates: (a) 0.4Q, (b) 0.6Q, (c) 0.8Q, (d) 1.0Q, (e) 1.2Q, (f) 1.4Q, and (g) 1.6Q

E. Overall Assessment and Design Implications

Across all variations, wind speed has the strongest effect on the absolute power output, which reaches a maximum of 139.87 W at 20 m/s. This holds for the ranges examined here, and it comes with a falling power coefficient because the effective TSR departs from its design value. The expansion ratio improves torque and power through flow augmentation, with performance saturating at ER ≈ 2.0 (35.74 W; C_P = 1.664), a 23.3% gain over the straight duct; the marginal gain up to ER = 2.5 does not justify the increased separation risk. The flow-rate series shows a consistent increase in power accompanied by a decrease in C_P, i.e., a trade-off between output and conversion efficiency.

Taken together, the most favorable configuration within the studied ranges combines an expansion ratio of about 2.0, a wind speed of roughly 4.5–7 m/s (the range in which the TSR stays close to the design value), and a relative flow rate of 1.0–1.6Q_{design}. In this configuration the diffuser augments the flow effectively without a dominant separation zone, and the turbine runs near its design TSR, so conversion efficiency is retained. This wind-speed window is highly relevant to Indonesia, where low-wind conditions prevail.

Several limitations should be acknowledged. The simulations are steady-state, use a single benchmark geometry, and keep the rotor speed fixed; no bare-turbine case was simulated, so the gain relative to an unducted rotor is not quantified here; the coefficients use the free-stream rather than the local rotor-plane velocity; and validation relies on one operating point of a published numerical dataset rather than on measurements. These points are taken up in Section VII.

Copyright © 2026 CJESR All Rights Reserved

Current Journal of Engineering and Science Research
Volume 3, Issue 11, pp 16-25, November 2026
ISSN (online): 3049-1738
DOI: https://doi.org/10.47001/CJESR/2026.311003
Available Online at https://www.cjesr.com

VI. CONCLUSION

CFD simulations of a ducted wind turbine lead to the following conclusions:

1) Wind speed has a significant effect on turbine performance. Raising the wind speed from 3 to 20 m/s increased the torque from 0.7838 to 3.6264 N·m and the power from 30.23 to 139.87 W, while the power coefficient fell because the fixed rotor speed drove the TSR away from the design value of 3. The most efficient operation lies at about 4.5–7 m/s.
2) The diffuser expansion ratio influences the flow augmentation at the rotor. Increasing ER from 1.0 to 2.0 raised the torque from 0.7516 to 0.9268 N·m and the power from 28.99 to 35.74 W (+23.3%); beyond ER = 2.0 the gain was marginal (35.79 W at ER = 2.5), and the contours indicate incipient flow separation, so ER ≈ 2.0 is the effective optimum.
3) The flow rate affects power and efficiency in opposite directions. From 0.4Q to 1.6Q (1.8–7.2 m/s), the torque rose from 0.7275 to 1.0223 N·m and the power from 28.06 to 39.43 W, whereas the power coefficient decreased markedly. Meaningful coefficients occur at 1.0–1.6Q.
4) Within the ranges studied, wind speed is the parameter with the largest effect on power output. The recommended configuration is ER ≈ 2.0, a wind speed of 4.5–7 m/s, and Q/Q_{design} = 1.0–1.6.
5) Overall, the diffuser enhances energy extraction by accelerating the flow at the rotor plane, which makes ducted turbines a promising option for regions with low-to-moderate wind speeds.

VII. FUTURE SCOPE

Future work should (i) repeat the wind-speed and flow-rate sweeps at a constant tip speed ratio so that performance is not confounded with off-design operation; (ii) include a bare-turbine baseline to quantify the augmentation directly; (iii) report a mesh-independence study and use unsteady (sliding-mesh) or scale-resolving simulations; (iv) compute the power coefficient from the area-averaged velocity at the rotor plane; (v) extend the geometric study to expansion ratios beyond 2.5 and to flange height, diffuser length, and flange angle; and (vi) validate the model in a wind tunnel and consider realistic atmospheric boundary-layer wind profiles and turbulence intensities.

ACKNOWLEDGEMENT

The authors thank their fellow students in the Mechanical Engineering Study Program, Universitas Diponegoro, for their support. This research received no specific grant from any funding agency in the public, commercial, or not-for-profit sectors.

REFERENCES

[1] Global Wind Energy Council, "Global Wind Report 2025," *GWEC, Brussels, Belgium*, Apr. 2025.
[2] P. Sadorsky, "Wind energy for sustainable development: Driving factors and future outlook," *Journal of Cleaner Production*, vol. 289, 2021.
[3] C. Jung, "Recent development and future perspective of wind power generation," *Energies*, vol. 17, no. 21, 2024.
[4] PT PLN (Persero), Rencana Usaha Penyediaan Tenaga Listrik (RUPTL) 2025–2034, approved by Minister of Energy and Mineral Resources Decree No. 188.K/TL.03/MEM.L/2025. Jakarta, Indonesia, 2025.
[5] N. A. Pambudi et al., "The future of wind power plants in Indonesia: Potential, challenges, and policies," *Sustainability*, vol. 17, no. 3, 2025.
[6] T. Burton, D. Sharpe, N. Jenkins, and E. Bossanyi, Wind Energy Handbook, *3rd ed. Chichester, U.K.: Wiley*, 2021.
[7] D. A. Teklemariyem, N. H. R. Syed, and P. B. Dao, "CFD-driven design optimization of corrugated-flange diffuser-integrated wind turbines for enhanced performance," *Energies*, vol. 18, no. 17, 2025.
[8] N. Shambira, G. Makaka, and P. Mukumba, "Velocity augmentation model for an empty concentrator-diffuser-augmented wind turbine and optimisation of geometrical parameters using surface response methodology," *Sustainability*, vol. 16, no. 4, 2024.
[9] N. Bekele and W. Bogale, "Parametric study of a diffuser for horizontal axis wind turbine power augmentation," *AIMS Energy*, vol. 7, no. 6, pp. 841–856, 2019.
[10] S. Sridhar et al., "Aerodynamic comparison of slotted and non-slotted diffuser casings for diffuser augmented wind turbines (DAWT)," *Renewable and Sustainable Energy Reviews*, vol. 161, 2022.
[11] M. A. Rahmatian, P. Hashemi Tari, M. Mojaddam, and S. Majidi, "Numerical and experimental study of the ducted diffuser effect on improving the aerodynamic performance of a micro horizontal axis wind turbine," *Energy*, vol. 245, 2022.
[12] I. H. Kim, B. R. Kim, Y. J. Yang, and S. J. Jang,

Copyright © 2026 CJESR All Rights Reserved

Current Journal of Engineering and Science Research
Volume 3, Issue 11, pp 16-25, November 2026
ISSN (online): 3049-1738
DOI: https://doi.org/10.47001/CJESR/2026.311003
Available Online at https://www.cjesr.com

"Parametric study on ducted micro wind energy harvester," *Energies*, vol. 15, no. 3, 2022.

[13] A. T. Nile, M. Emam, S. Ookawara, and S. A. Nada, "Performance prediction of a small-scale diffuser-augmented wind turbine with and without an inlet nozzle: A 2D and 3D analysis," *Energy Conversion and Management*, vol. 327, 2025.

[14] A. A. Firoozi, F. Hejazi, and A. A. Firoozi, "Advancing wind energy efficiency: A systematic review of aerodynamic optimization in wind turbine blade design," *Energies*, vol. 17, no. 12, 2024.

[15] H. Hamid and R. M. Abd El Maksoud, "A numerical assessment of the heterogeneous effects of innovative shroud profiles for horizontal axis wind turbine," *Heliyon*, vol. 11, no. 2, 2025.

[16] T. A. Jauhar et al., "Effect of flanged diffuser divergence angle on wind turbine: A numerical investigation," *PLoS ONE*, vol. 18, no. 6, 2023.

[17] M. R. Behery, D. H. Didane, and B. Manshoor, "Optimization of flanged diffuser for small-scale wind power applications," *CFD Letters*, vol. 16, no. 7, pp. 54–70, 2024.

[18] A. Rachman, A. Johnstone, and B. Kosasih, "The effects of shape and size on duct-augmented horizontal axis turbine performance," *Wind Engineering*, vol. 45, no. 4, pp. 953–972, 2021.

[19] Y. Nakayama, "Fundamentals of flow," in Introduction to Fluid Mechanics. *Oxford, U.K.: Butterworth-Heinemann*, 2018, pp. 51–65.

[20] F. R. Menter, "Two-equation eddy-viscosity turbulence models for engineering applications," *AIAA Journal*, vol. 32, no. 8, pp. 1598–1605, 1994.

Citation of this Article:

Nazaruddin Sinaga, Dwi Basuki Wibowo, & Rendy Augustino Sam. (2026). CFD Investigation of the Effects of Wind Speed and Duct Geometry on the Performance of a Ducted Wind Turbine for Energy Efficiency. *Current Journal of Engineering and Science Research*. 3(11), 16-25. Article DOI: https://doi.org/10.47001/CJESR/2026.311003

***** End of the Article *****

Copyright © 2026 CJESR All Rights Reserved